Paper Number: **3902**

Title: **A Biaxial-Bending Test to Observe the Growth of Interacting Delaminations in a Composite Laminate Plate**

Authors: Mark McElroy
Wade Jackson
Mark Pankow

(FIRST PAGE OF ARTICLE – *align this to the top of page – leave space blank above ABSTRACT*)

ABSTRACT

It is not easy to isolate the damage mechanisms associated with low-velocity impact in composites using traditional experiments. In this work, a new experiment is presented with the goal of generating data representative of progressive damage processes caused by low-velocity impact in composite materials. Carbon fiber reinforced polymer test specimens were indented quasi-statically such that a biaxial-bending state of deformation was achieved. As a result, a three-dimensional damage process, involving delamination and delamination-migration, was observed and documented using ultrasonic and x-ray computed tomography. Results from two different layups are presented in this paper. Delaminations occurred at up to three different interfaces and interacted with one another via transverse matrix cracks. Although this damage pattern is much less complex than that of low-velocity impact on a plate, it is more complex than that of a standard delamination coupon test and provides a way to generate delamination, matrix cracking, and delamination-migration in a controlled manner. By limiting the damage process in the experiment to three delaminations, the same damage mechanisms seen during impact could be observed but in a simplified manner. This type of data is useful in stages of model development and validation when the model is capable of simulating simple tests, but not yet capable of simulating more complex and realistic damage scenarios.

INTRODUCTION

As the prevalence of composite materials increases in the aerospace industry, so do certain costs that are associated specifically with using these types of materials. One of these costs is associated with composite laminates' susceptibility to damage from transverse loads, such as impacts on the surface of a panel. As a result, composite structures usually do not incorporate damage tolerance into their design. This can lead to structural designs that are overly conservative and inefficient. Another

cost driver is a lack of robust and reliable damage simulation tools for composites. Without such tools, certification of composite structures relies almost entirely on testing [1, 2]. If reliable damage simulation tools were available for composites, certain tests could be replaced with analysis, and damage tolerance could be integrated into a design process in a more affordable way. The potential result of developing such tools would be cheaper and more efficient composite structures [3, 4, 5].

A challenge for developing numerical damage simulation tools for composites is that damage processes in laminates can be very complex, consisting of perhaps dozens of interacting delaminations and matrix cracks in a three-dimensional network. A common cause of this type of damage is low-velocity impact (LVI). Figure 1 is a section view of typical LVI damage in a laminate. The development of simulation models that can predict a complex three-dimensional network of cracks such as this in a reliable manner has had some success to date, but has proven to be difficult [2, 6].

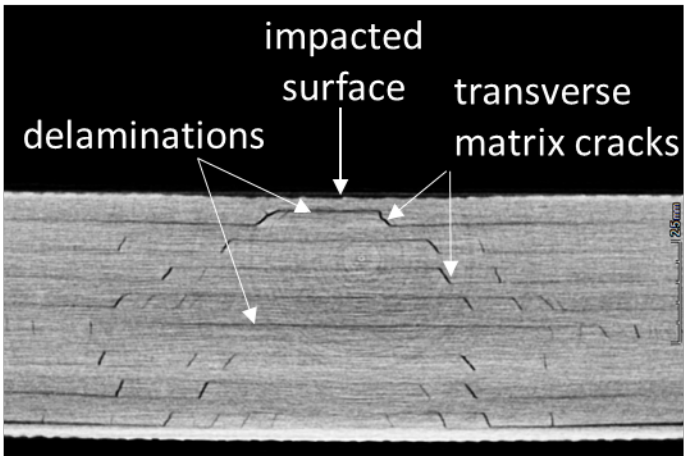

Figure 1. Typical impact damage in a composite laminate.

The approach commonly used when creating a new simulation model is to start with simple damage problems, such as standard delamination coupon models, and develop the model incrementally by increasing problem complexity. In order to use this approach, experimental validation data are needed at each stage of problem complexity.

Validation data for simple coupon-sized unidirectional laminate structures, often obtained from ASTM standard tests [7-9], are available from several sources (e.g., [10,11]). Damage documented in these tests is confined to one ply interface and does not replicate the complex damage that can result from LVI (see Figure 1).

A slightly more complex damage process may include transverse matrix cracking. Ratcliffe et al.'s delamination-migration experiment is well documented and consists of a delamination that grows from an implanted crack starter, then migrates to a new interface via a transverse matrix crack, and then continues growth at that new interface [12]. The experiment is useful in model development and validation, as it isolates a specific damage mechanism; however, it is designed to do only that, not to represent a realistic damage scenario such as LVI.

Consideration of damage problems of medium complexity, in between that of the delamination-migration experiment and that of LVI, is useful in model development. Medium complexity in this context may be defined as progressive damage in a laminate that involves no more than two or three delaminations at different interfaces.

The goal of the research described in this paper is to generate experimental validation data for laminate damage processes that consist of no more than three delaminations interacting with one another via transverse matrix cracks. A new quasi-static indentation experiment is developed to achieve this goal. The data from this quasi-static test are thought to be applicable to progressive damage processes that occur as a result of LVI, based on previous work showing behavioral equivalence between the two types of loads [13-15].

EXPERIMENT DESCRIPTION

Overview

An experiment was designed to create a progressive damage process that consisted of multiple delaminations growing at different interfaces and interacting with one another via transverse matrix cracks in a carbon fiber reinforced polymer (CFRP) specimen. The specimens, square in shape and containing a quarter circle preexisting crack in one corner, were clamped on the two edges opposite the preexisting crack. A quasi-static indentation load was applied to the corner of the specimen containing the preexisting crack. These loading and boundary conditions result in a biaxial-bending state of deformation in the specimen. The test is illustrated in Figure 2.

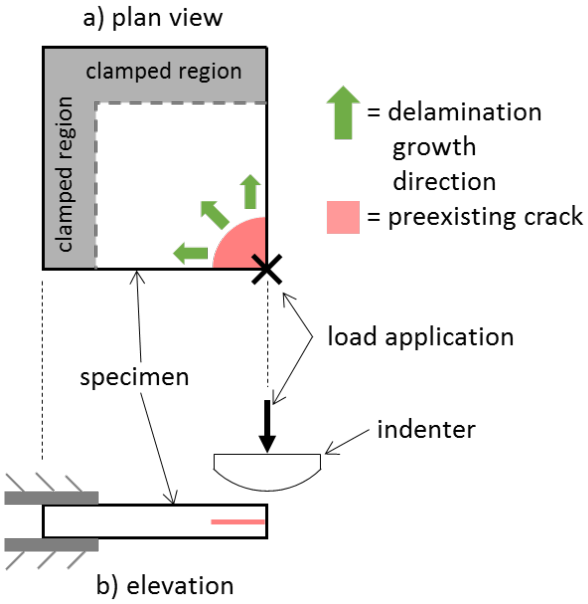

Figure 2. Test schematic.

Canturri et al. performed a test that was configured in much the same way [16]. The primary difference between Canturri et al.'s test and the test described herein is the biaxial-bending deformation. The biaxial-bending state, combined with the quarter circle geometry of the preexisting crack, results in a damage pattern that grows radially rather than linearly, as would occur under a state of bending about a single axis. The implications of the biaxial-bending are explored and discussed further in the following section.

Test specimen

The CFRP test specimens were manufactured using an IM7/8552 carbon fiber-epoxy material system and cured according to the manufacturer's instructions [17]. The specimen geometry is described in Figure 3. Two layups were tested and the results are presented in this paper. The two layups selected were chosen so that migration could be studied through both 90° fibers and -45° fibers. Square plates (105 mm × 105 mm) were manufactured with a circular Polytetraflouroethylene (PTFE) insert (13 micron thick, 10 mm radius) located at the center point of the plate at the interface designated by "T" in Figure 3. The plates were then cut symmetrically about the center point to create four 52.5 mm × 52.5 mm square test specimens, each with a quarter circle PTFE insert in one corner.

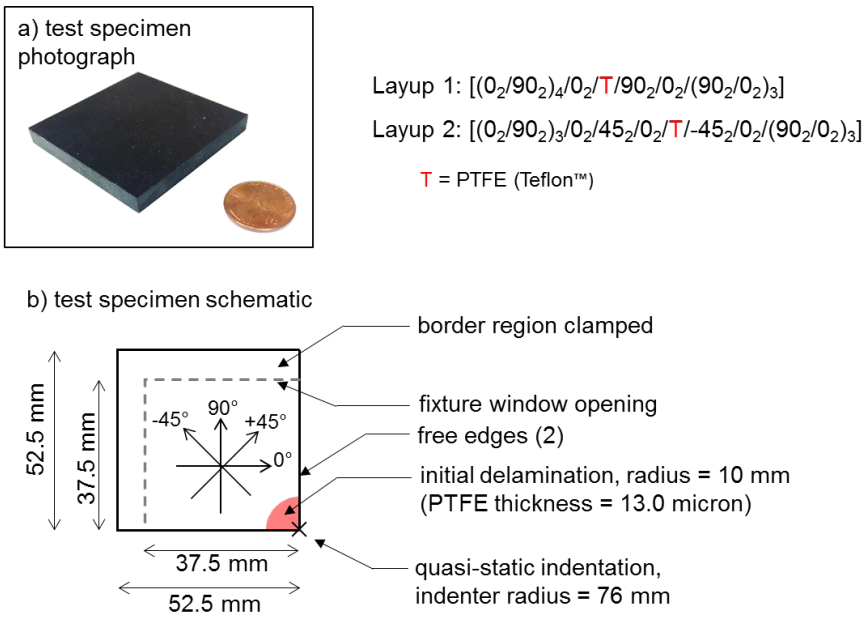

Figure 3. Test specimen description.

Test setup

The test setup is shown in Figures 4a and 4b. A square CFRP specimen was clamped in one corner of a steel picture frame impact test fixture. Four bolts, one in each corner of the fixture, were tightened to a torque of 9.5 N·m, resulting in a clamp condition that held the specimen firmly in the fixture but was not so tight as to damage the specimens. Guide plates on the lower clamping surface, seen in Figure 4c, ensured that all specimens were always in the same position when placed in the clamp. A 22.2kN servo-hydraulic test frame was used to apply the quasi-static loads at a rate of 0.127 mm/min. Load was applied vertically to the free corner of the specimen using a 76 mm diameter steel nose.

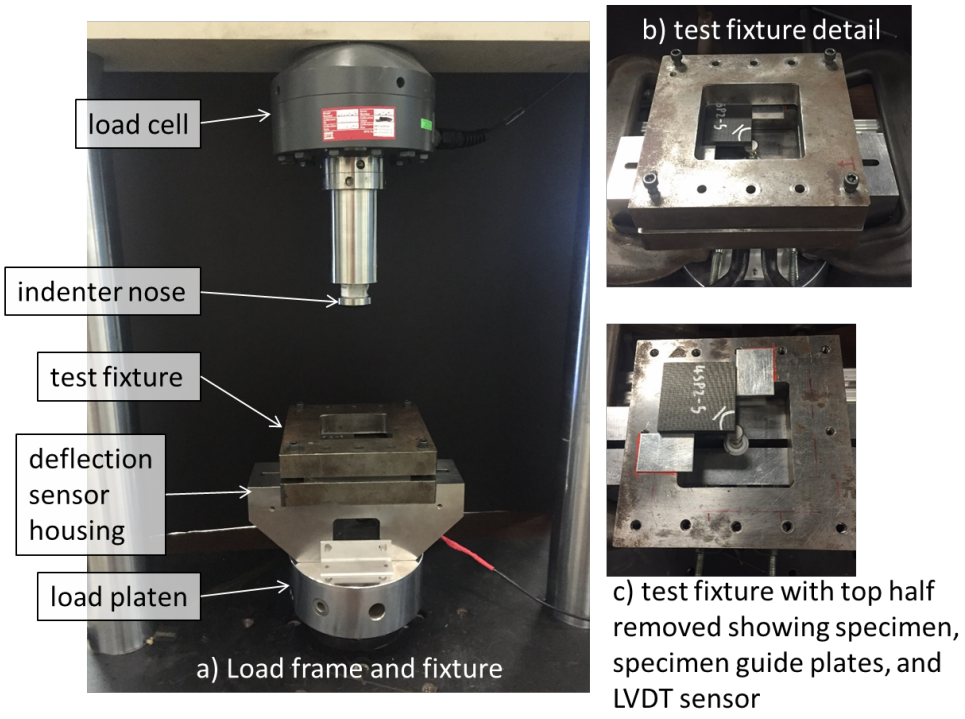

Figure 4. Experiment setup.

Multiple quasi-static load cycles were carried out for each test and ultrasonic (UT) and X-ray computed tomography (CT) scans were performed on the specimens after each load cycle so that damage could be documented progressively. The number of load cycles applied to a given specimen varied between one and eleven. In certain tests, several "pre-damage" load/scan cycles were performed by applying a load below that of delamination initiation to determine if any small amount of damage was occurring prior to delamination. In some instances, a small amount of delamination is evident in the final "pre-damage" load cycle. Test specimen deflection was measured from the bottom specimen surface using a mechanical transducer placed in a frame below the test fixture. The mechanical transducer was used to measure the true deflection of the specimen, absent any influence from test stand or fixture deformation.

TEST RESULTS AND DISCUSSION

Layup 1: $[(0_2/90_2)_4/0_2/T/90_2/0_2/(90_2/0_2)_3]$

Force-displacement data for all of the Layup 1 specimens tested are plotted in Figure 5. The curves from the tests where multiple load cycles were performed are plotted by showing only the regions from each load cycle that do not overlap with another. This manner of plotting multiple load cycles is illustrated in Figure 6, using specimen XP3-2 as an example. In Figure 5, for specimen XP3-6, the maximum forces for several "pre-damage" load cycles (as described in the Test setup section) are identified by points *i*-*iv*.

Damage behavior is consistent between all tests, though some variance can be seen in the force required for damage initiation (i.e., variance in the toughness at the PTFE boundary). After an initially elastic regime, the subsequent damage growth stability was dependent on how much strain energy had built up before initiation. In cases where the critical force was higher, initiation was followed first by unstable delamination growth and then eventually continued stable growth. In cases where the critical force was lower, damage growth was stable throughout. Dashed portions of the curve in all of the force-displacement plots in this paper are used in instances where, due to brief unstable growth and a resulting rapid deflection for a small amount of time, the deflection transducer lost contact with the specimen.

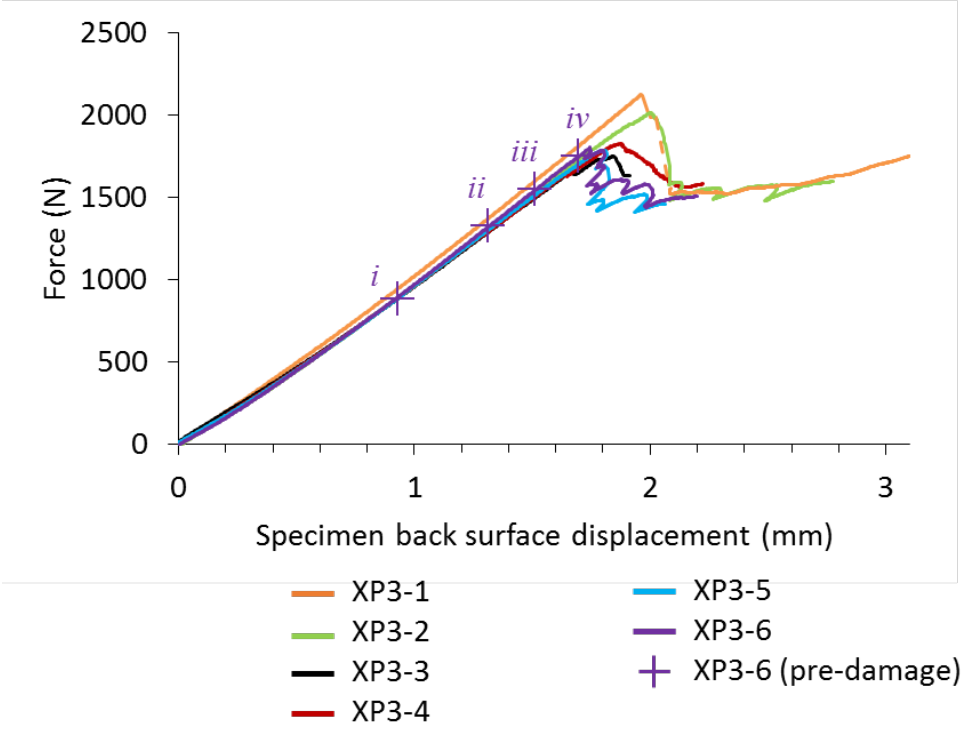

Figure 5. Force-displacement data from Layup 1.

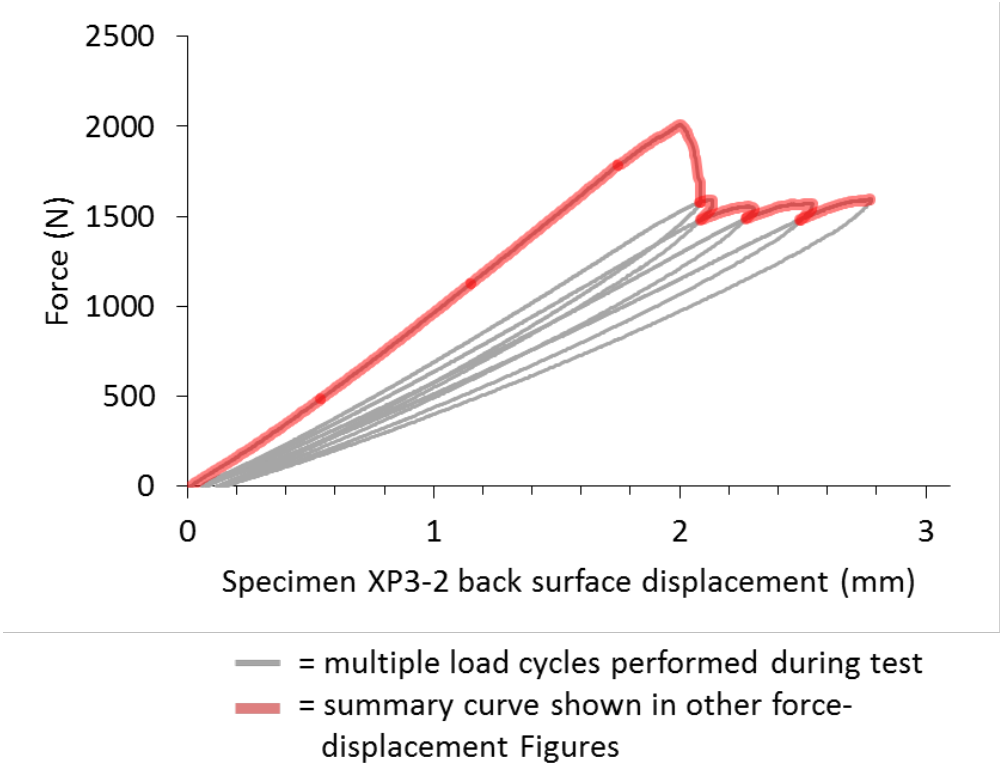

Figure 6. Multiple load cycles and summary force-displacement curve.

UT scans are shown in Figure 7 from the "top" (i.e., loaded) side of test specimen XP3-6 for loading conditions from "pre-damage" load *iv,* just as delamination begins, through Load 7, after delamination initiation and migration. The bottom surfaces of the specimens were also scanned to confirm that no additional delaminations were present and were hidden in the shadow of those shown in the figure. The damage shown in Figure 7 is representative of damage seen in all of the Layup 1 specimens. Two delaminations grew during the test from the PTFE insert, at two interfaces identified in Figure 7. The scan labeled "Load *iv*" shows the PTFE quarter-circle insert, as well as the first instance of delamination growth at the region above the PTFE boundary near the right hand side of the specimen.

An isometric diagram of the specimen and matrix cracking is shown in Figure 8. In the region of the PTFE border near the lower edge of the specimen, the delamination migrated almost immediately down to interface 1 and then continued to grow at that interface, bounded below by 0° fibers. In the region of the PTFE near the right hand edge of the specimen, the delamination grew in the 90° direction and remained at that same interface (interface 0) bounded below by 90° fibers. Both delaminations grew simultaneously along a transverse matrix crack through the 90° plies between interface 0 and interface 1 as shown in Figure 7. The transverse matrix crack began as the initial migration from the PTFE film.

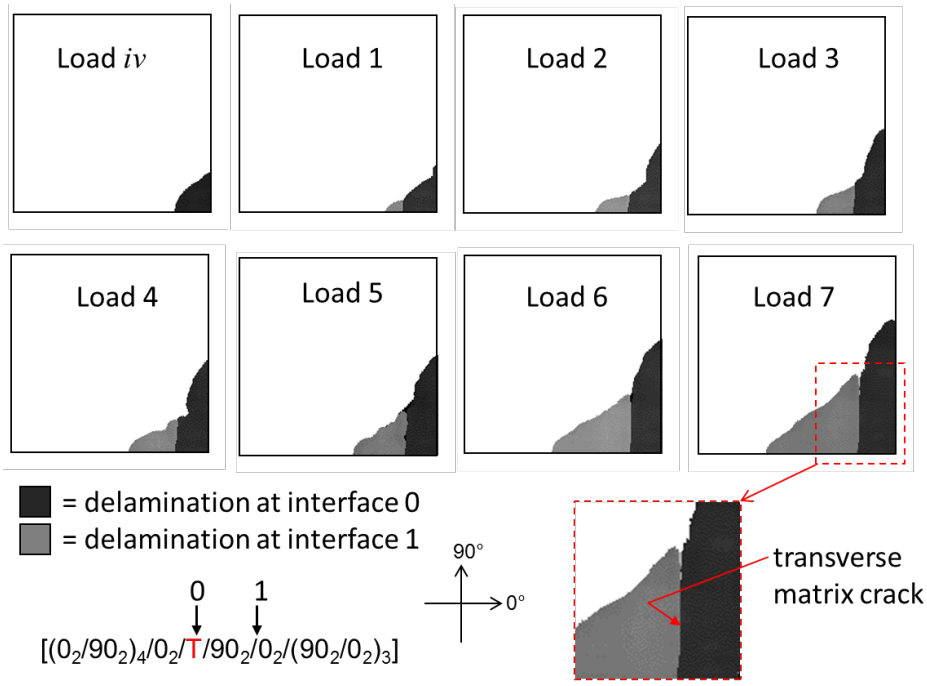

Figure 7. UT scans of damage in Layup 1.

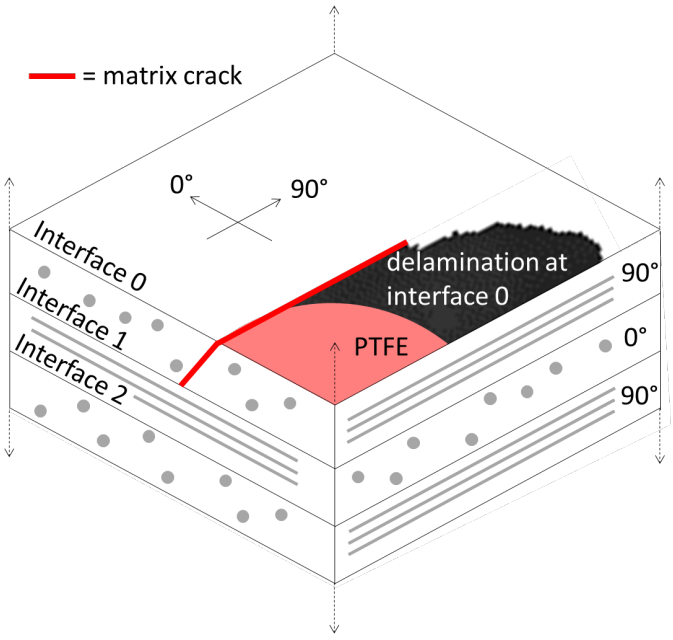

Figure 8. Matrix cracking diagram for Layup 1.

The delamination-migration mechanism seen in the test was studied by Ratcliffe et al. [12]. In their work, delamination-migration was explained by demonstrating that the sign of the shear stress at a delamination front dictates an out-of-plane directional growth tendency. More specifically, the sign of the shear stress at the delamination front dictates the orientation of a series of Mode I microcracks that precede a delamination front as it is growing. If the growth of the microcracks is oriented towards, and reaches, fibers that have an orientation that arrests their growth (that is,

further growth of the microcracks would require breaking fibers), they will coalesce into a macrocrack, be redirected along the bounding fiber direction, and form a delamination. If the microcracks are not contained by bounding fibers, they still may coalesce, but instead of forming a delamination, they form a transverse matrix crack that grows in between fibers through a ply. After formation of the transverse crack, the delamination may resume at a new interface once a new fiber orientation is reached that arrests the transverse growth (i.e., migration). An example is shown in Figure 9 illustrating delamination-migration in a simple [0/90/0] laminate.

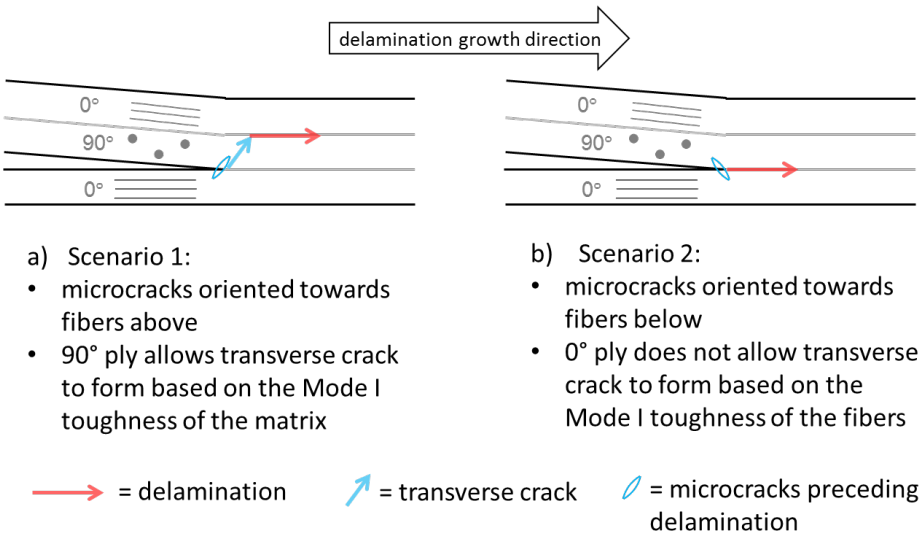

Figure 9. Illustration of conditions for delamination migration in a [0/90/0] layup.

In the biaxial-bending specimens, the deformation and resulting shear stress sign are such that the microcrack growth is always pointing towards the ply below. Additionally, past observations suggest that the microcracks are oriented perpendicularly to the direction of delamination growth about the transverse axis [18, 19]. Because of the biaxial-bending nature of the test, and because of the quarter circle PTFE shape, the delamination growth direction spans all possible angles relative to the bounding fibers in the ply below. This is illustrated in Figure 10a, where $0° \leq \alpha \leq 90°$ and microcracks (in plan view) are illustrated by dashed red lines. In the region of the PTFE boundary near the lower edge of the specimen, where the delamination growth direction is perpendicular to the 90° fibers below, the microcrack orientation is perpendicular to the delamination growth direction and parallel to bounding fibers. Therefore, in this case, the microcracks could propagate easily through the 90° plies in the form of a matrix crack and the delamination migrated to interface 1. In the region of the PTFE near the right hand side of the specimen, however, the delamination growth direction is in line with the 90° bounding fibers and the microcrack growth direction is perpendicular to the bounding fibers. As a result, the microcracks cannot coalesce and grow through the ply as a matrix crack and instead coalesce at interface 0 as delamination growth occurs.

Finally, for directions of delamination growth that are in between perpendicular and parallel to bounding fibers, there was a certain range of α where several transverse cracks formed and migration began; however, only the first transverse crack to form actually completed the migration process and led to continued delamination on the

new interface. This can be seen in the CT scans of one specimen, shown in Figures 10b and 10c. More investigation is warranted on understanding the occurrence of migration for delamination growth directions that are neither parallel nor perpendicular to bounding fibers.

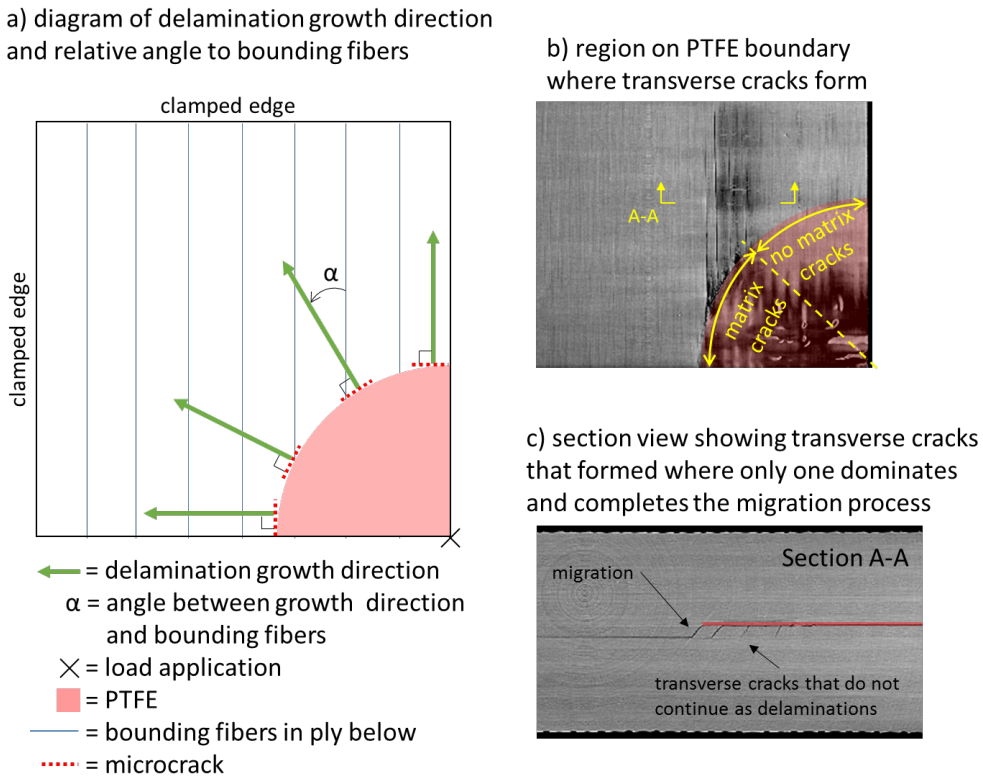

Figure 10. Delamination growth and migration detail (CT images from specimen XP3-6).

A final observation regarding migration is that the first transverse matrix crack (i.e., the one that ultimately led to migration) was seen to form at "pre-damage" load *i* in specimen XP3-6, well before the initiation of delamination growth. Computed tomography (CT) images are shown in Figure 11 that were captured at "pre-damage" points along the load curve as identified in Figure 5 for specimen XP3-6. This matrix cracking is not evident from a simple inspection of the force-displacement curve, which indicates that the energy required to form this crack is very small and possibly negligible in the context of a numerical simulation.

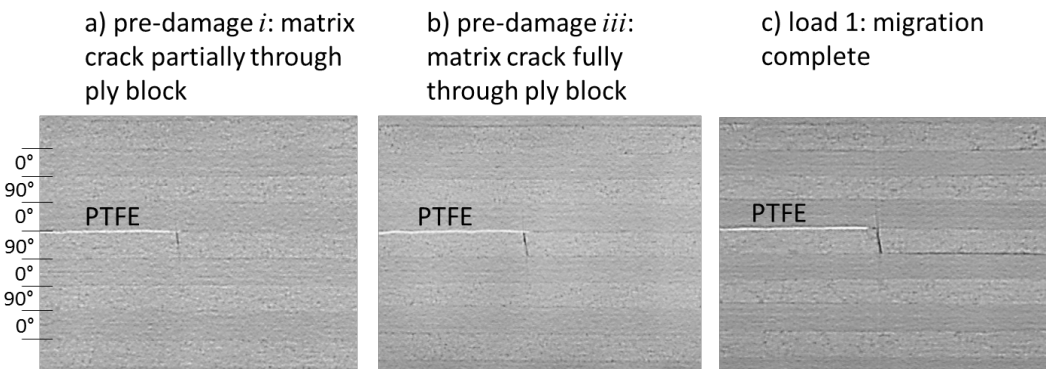

Figure 11. CT images of transverse matrix cracks forming incrementally before delamination growth initiation (specimen XP3-6).

Layup 2: $[(0_2/90_2)_3/0_2/45_2/0_2/T/-45_2/0_2/(90_2/0_2)_3]$

Force-displacement data for all of the Layup 2 specimens tested are plotted in Figure 12. As in the Layup 1 data, the curves from tests where multiple load cycles were performed are plotted by showing only the regions from each load cycle that do not overlap with another (see Figure 6). For specimen 45P2-6, the maximum force for several "pre-damage" load cycles are identified by points *i*-*v*. The overall force-displacement data are similar to that of the Layup 1 tests, although less variance in the critical force was seen.

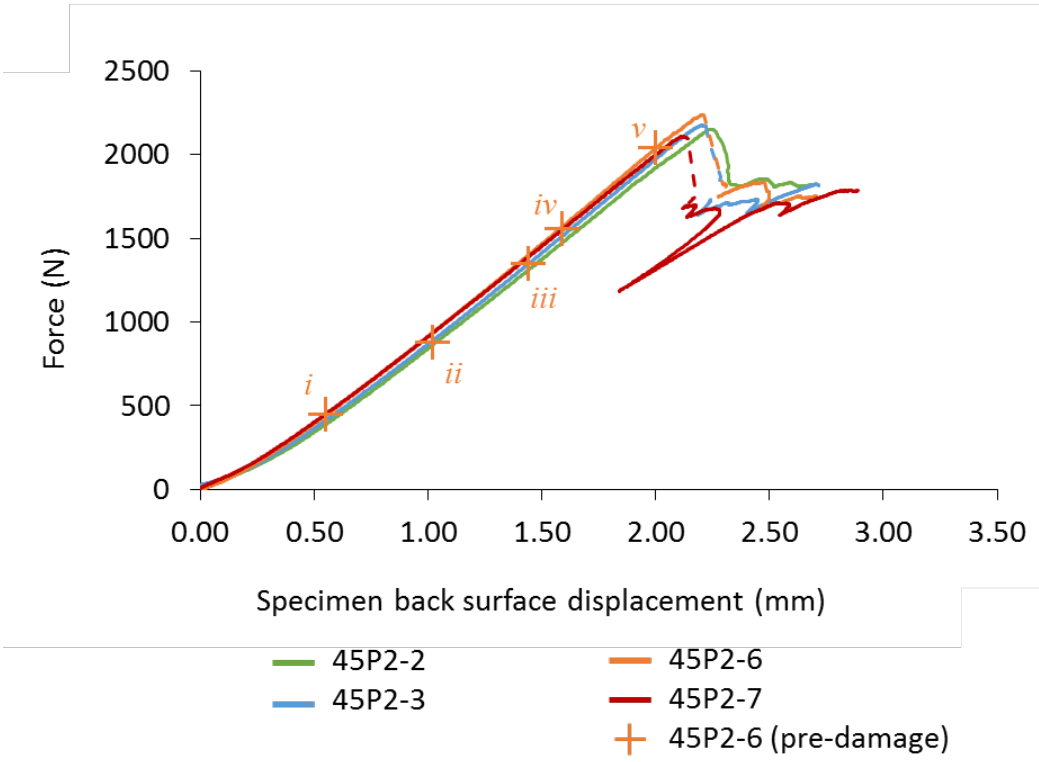

Figure 12. Force-displacement data from Layup 2.

UT scans are shown in Figure 13 from the "top" (i.e., loaded) side of specimen 45P2-6, which underwent six load cycles after the "pre-damage" loads. The damage shown is representative of damage seen in all of the Layup 2 specimens. Delaminations grew during the test from the PTFE insert at the three interfaces defined in Figure 13. In this layup, delamination emanating from the central region of the PTFE boundary remained at interface 0 and was bound by the -45° fibers below. In the region of the PTFE boundary near the lower edge of the specimen, the delamination migrated through the -45° plies and then continued growth in interface 1, bounded by 0° fibers below. In the region of the PTFE boundary near the right hand side of the specimen, the delamination migrated through both the -45° and 0° ply groups and then continued growth at interface 2, bounded by 90° fibers below. Additionally, in this region, as seen in Figure 13 at Load 3, the delamination at interface 0 has grown such that it obscures the already existing delamination below at interface 2. An isometric diagram of the matrix cracking is shown in Figure 14.

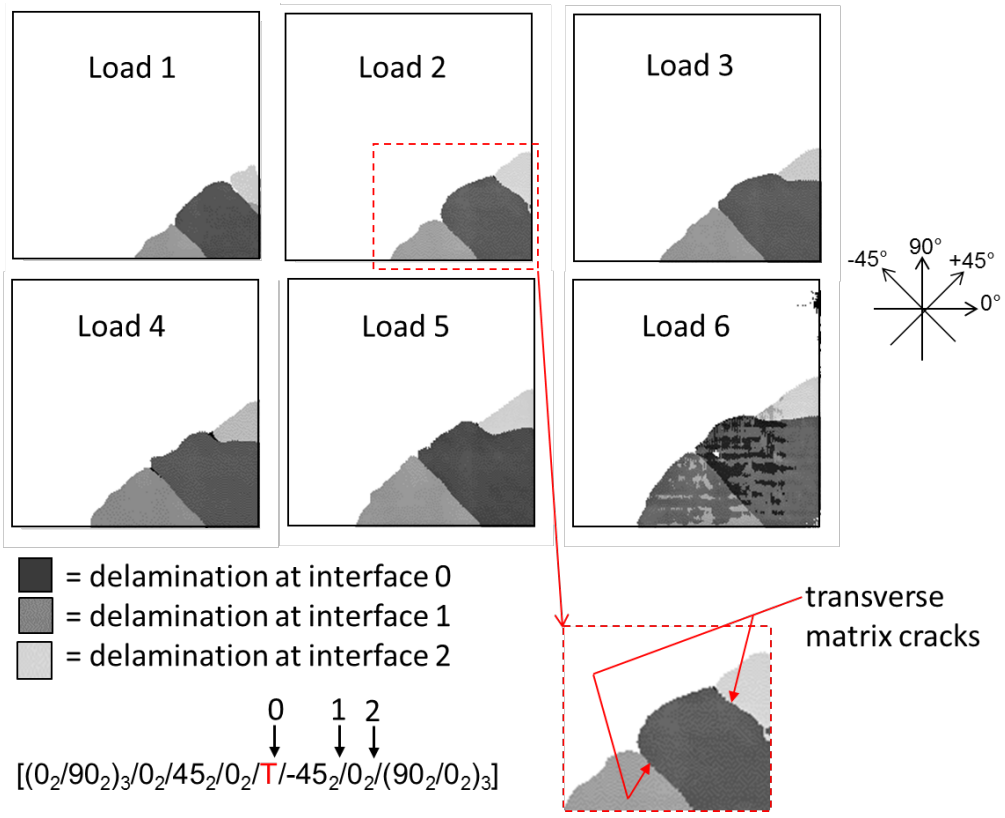

Figure 13. UT scans of damage in Layup 2.

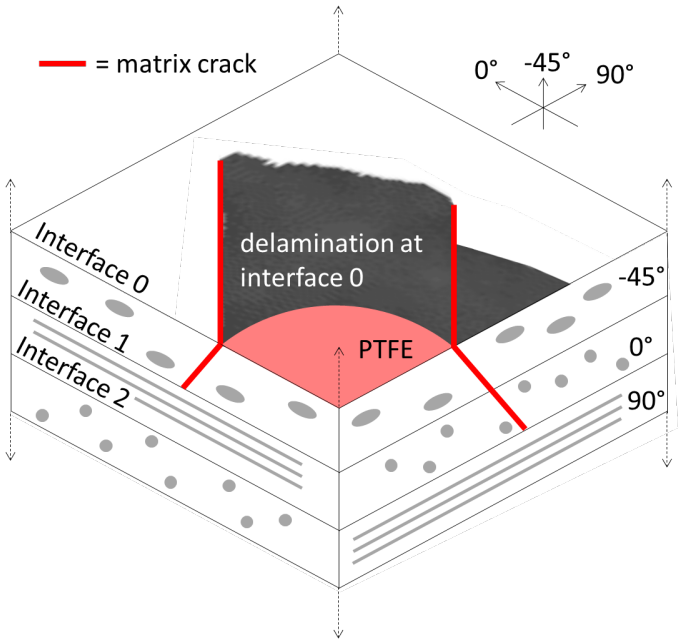

Figure 14. Matrix crack diagram for Layup 2.

The delaminations at interface 1 and interface 0 share a boundary consisting of a transverse matrix crack. The boundary that the delamination at interface 0 shares with that of interface 2 is more complex. From the interface 0, a transverse matrix crack extends down through the -45° fibers to interface 1 ("0-1 crack"). For this crack to proceed further on the same path through the thickness down to interface 2, fibers would have to be broken, which did not occur. Instead, a series of smaller disconnected transverse matrix cracks through the 0° ply below interface 1 formed along the path of the 0-1 crack. This is shown in the CT images in Figure 15. The damage pattern seen in the Layup 2 specimens is thought to be particularly useful for model development and validation, as it contains two types of interactions between delaminations: (1) a clean matrix crack through fibers of the same orientation and (2) a "staggered migration" consisting of a system of matrix cracks in different layers and at different orientations, but following the same global path through the specimen.

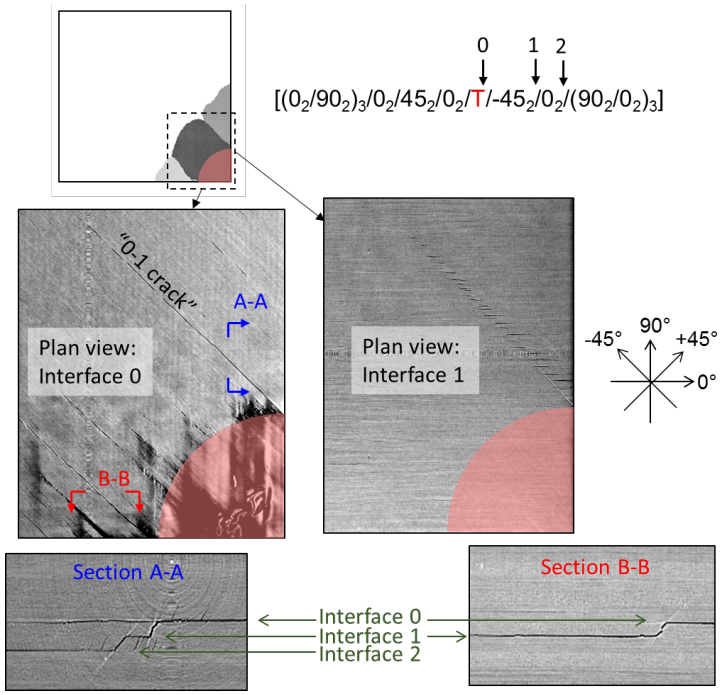

Figure 15. CT scans showing "staggered migration".

CONCLUSION

An experiment has been introduced that produces, within a limited number of plies, controlled delamination, matrix cracking, and delamination-migration. The level of damage complexity was intended to be greater than that of delamination coupon tests, but less than that of LVI on a plate. By limiting the damage process in the experiment to three delaminations, the same damage mechanisms seen during impact can be recreated in a simplified manner. The experimental data may be used for both model validation and simply to understand better the common damage mechanisms seen in progressive damage processes in laminates. The experimental data are representative of damage seen in LVI after initiation has occurred.

The test consisted of a square laminate plate that was clamped on two adjacent edges. At the free corner of the plate, where a PTFE insert in the layup was located, a quasi-static indentation load was applied. Delaminations grew from the PTFE insert on up to three different interfaces and interacted with one another via transverse matrix cracks. Two different layups were tested, and in both layups, transverse matrix cracks were seen to form well before the initiation of delamination. The formation of these cracks is not apparent on the force-displacement plots, indicating that the energy associated with their growth is small and perhaps negligible in the context of a numerical simulation model.

Ultrasonic and computed tomography scans were performed on the specimens to characterize damage. The damage mechanisms that occurred in the test that are thought to be particularly relevant were delamination, delamination-migration, and the interaction of multiple delaminations via matrix cracks. In some cases, adjacent delaminations were joined by a transverse matrix crack through a block of commonly oriented plies. In other cases, adjacent delaminations were joined by a path of a series of disconnected transverse matrix cracks through two ply blocks of differing

orientation (staggered migration). More investigation is warranted on the formation of transverse matrix cracks, especially in cases where the delamination growth direction is in between parallel and perpendicular to the bounding fiber direction.

REFERENCES

1. Hinton, M.J., A.S. Kaddour, and P.D. Soden. 2004. "The world-wide failure exercise: Its origin, concept, and content," *Failure criteria in fiber reinforced polymer composites: the world wide failure exercise*, pp 2-28. Elsevier, Amsterdam.
2. Rose, C.A., C.G. Davila, and F.A. Leone. 2013. *Analysis methods for progressive damage of composite structures, NASA/TM 2013-218024*. NASA.
3. Allison, J. 2011. "Integrated Computational Materials Engineering: A Perspective on Progress and Future Steps," *JOM: The Journal of the Minerals, Metals and Materials Society*, **63**(4) pp. 15-18.
4. Allison, J., Backman, D., and Christodoulou, L. 2006. "Integrated Computational Materials Engineering: A New Paradigm for the Global Materials Profession," *JOM: The Journal of the Minerals, Metals and Materials Society*, **58**(11) pp. 25-27.
5. Apelian, D. 2008. "Integrated Computational Materials Engineering (ICME): A 'model' for the Future?," *JOM: The Journal of the Minerals, Metals and Materials Society*, **60**(7) pp. 9-10.
6. Liu, P.F. and J.Y. Zheng. 2010. "Recent developments on damage modeling and finite element analysis for composite laminates: a review," *Materials and Design*, 31(8):795-805.
7. ASTM D5528-01 "Standard Test Method for Mode I Interlaminar Fracture Toughness of Unidirectional Fiber-Reinforced Polymer Matrix Composites," *2004 Annual Book of ASTM Standards,* Vol.15.03.
8. ASTM D7905 "Standard Test Method for Determination of the Mode II Interlaminar Fracture Toughness of Unidirectional Fiber-Reinforced Polymer Matrix Composites," *2014 Annual Book of ASTM Standards,* Vol.15.03.
9. ASTM D6671M-04 "Standard Test Method for Mixed Mode I-Mode II Interlaminar Fracture Toughness of Unidirectional Fiber-Reinforced Polymer Matrix Composites," *2004 Annual Book of ASTM Standards,* Vol.15.03.
10. Paris, I., P.J. Minguet, and T. K. O'Brien. 2003. "Comparison of delamination characterization for IM7/8552 composite woven and tape laminates," In *Composite Materials: Testing and Design, Fourteenth Volume, STP 1436*. ASTM International.
11. Hansen, P. and R. Martin. 1999. *DCB, 4ENF and MMB delamination characterisation of S2/8552 and IM7/8552* (Contract Number N68171-98-M-5177). Materials Engineering Research Lab Ltd., Hertford (UK).
12. Ratcliffe, J.G., M.W. Czabaj, and T.K. O'Brien. 2013. *A test for characterizing delamination migration in carbon/epoxy tape laminates, NASA/TM-2013-218028*. NASA.
13. Sjoblom, P.O. and J.T. Hartness. 1988. "On low velocity impact testing of composite materials," *Journal of Composite Materials*, (22)1:30-52.
14. Jackson, W.C. and C.C. Poe Jr. 1993. "The use of impact force as a scale parameter for the impact response of composite laminates," *Journal of Composites Technology & Research,*15(4):282-292.
15. Choi, I.H. and C.S. Hong. 1994. "New approach for simple prediction of impact force history on composite laminates," *American Institute of Aeronautics and Astronautics*, (32)10:2067-2072.
16. Canturri, C., E.S. Greenhalgh, S.T. Pinho, & J. Ankersen. 2013. "Delamination growth directionality and the subsequent migration processes–The key to damage tolerant design," *Composites Part A: Applied Science and Manufacturing*, 54:79-87.
17. Hexcel. 2013. HexPly® 8552 Epoxy Matrix, product data. Hexcel. http://www.hexcel.com/Resources/DataSheets/Prepreg-Data-Sheets/8552_us.pdf
18. Greenhalgh, E.S. 2009. *Failure analysis and fractography of polymer composites*. Elsevier.
19. Canturri, C., E.S. Greenhalgh, S.T. Pinho. 2014. "The relationship between mixed-mode II/III delamination and delamination migration in composite laminates," *Composites Science and Technology* 105: 102-109.